American Journal of Engineering and Applied Sciences

Original Research Paper

Lagrange II Dynamics and that of Forces Exemplified on a Basic Robot, 2 DoF

Relly Victoria Virgil Petrescu

Department of Transportation, Traffic and Logistics, Bucharest Polytechnic University, Bucharest, Romania

Article history
Received: 02-06-2023
Revised: 27-06-2023
Accepted: 04-07-2023

Email: rvvpetrescu@gmail.com

Abstract: The paper presents two dynamic methods applied to a basic articulated robot, 2 DoF, the first being an original adaptation of the type II Lagrange equations and the second being a dynamic method based on the influence of the forces in the robot mechanism. Both methods are original, as they were designed and applied by the author to a 2 DoF basic robot. In the presentation, the results obtained by the two different dynamic methods are compared. It is interesting that although the differential equations obtained by the two methods presented in the paper are totally different, the results obtained with both models are very close in values. All simulations were processed with the help of Mathcad professional software.

Keywords: Kinematics, Nonlinear Dynamics, Forces, DoF Robot Mechanism, Type II Lagrange Equations

Introduction

It is known today that robots have the role of making human work easier, by taking over all difficult, repetitive, and tiring tasks, especially for the human central nervous system, dangerous, stressful, and long-lasting, in environments hostile to humans (polluted, chemical, radioactive, underwater, in space, on mined lands). Only thanks to them and the automation achieved with robots and or with robotic cells as well as with automatic processing machines, we managed to move to new industrial eras, in which today processing, assembly, and all operations in the factory are carried out exclusively with robots, automated, with amazing work speeds but also with a high quality of all the final products obtained, given that the work of the robots is permanent, on three shifts, possibly also on Saturdays, without meal breaks, without weekends, without holidays, without salary and or unions or claims. The most important aspect of automation is obviously the superior quality of the products processed by robots compared to those previously made with people, they are products obtained in much larger quantities and faster, without danger to people, at low competitive prices, and in much better conditions advantageous. It should be mentioned that the attempts of some highly trained workers to keep up with the robots have failed and, one by one, all the tasks that were still performed by humans have been replaced by robots.

The so-called danger of leaving us without jobs (which has long been the subject of trade union discussions) has naturally been solved over time by the transition of man to other easier, less dangerous, higher design jobs, concept, optimization, implementation, control, education, development, activities that can be carried out anywhere, anytime, with the desired breaks, remaining that the material value obtained immediately (now much higher) with robots, be distributed fairly to all the people who work, robots requiring only particular acquisition, implementation, maintenance costs, plus the necessary transport costs. In this way, the need for human labor could also be dispensed with on Sunday (which was sometimes used), a second weekly day off, Saturday and a short day on Friday could be introduced, and in the future, even the week of only four days' work for man. Man has freed himself from hard and health-hazardous work, now having the prospect of working in pleasant environments, only 4-5 days a week, with higher incomes and a much higher standard of living and security. The man has emancipated himself, managed to overcome his stage of working, moving to an evolved stage of thinking, to realize concepts and projects.

In the military field, robots, drones, and other automated components have been helping all types of military actions for a very long time today, no military operation is possible without the support of robots, drones, automation, and artificial intelligence.

Robots, drones, and artificial intelligence have penetrated almost all fields today, supported by wireless networks (increasingly developed), digitization, computerization, and automation, all evolving rapidly and permanently both by themselves and by the evolution of

increasingly modern electronic components (microchips and recently from February 2022 nanochips) but also of increasingly adapted materials (nanomaterials).

It should be emphasized that the essential role of robots is completely different, this being a historical role (today in full swing), namely "the conquest of cosmic space by humanity and the extension of the human species in the universe".

In computer science, Artificial Intelligence (AI) is the intelligence exhibited by machines, as opposed to the natural intelligence exhibited by humans and some animals. Today all machines have advanced artificial intelligence and both the software and the components of artificial thinking evolve very quickly. Modern machine capabilities broadly classified as AI include understanding human speech, competing at the highest level of strategy game systems, autonomous vehicles, and intelligent routing in content distribution networks, as well as military simulations.

The development of Metal-Oxide-Semiconductor (MOS) Very-Large-Scale Integration (VLSI), in the form of Complementary MOS (CMOS) technology, has allowed the number of MOS transistors to increase in digital electronics.

Automation has come a long way today, with the key role being played by DoF robots of various shapes and sizes.

We will remind you that a "Degree of Freedom" (DoF) in relation to robotic arms represents an independent joint that can provide the manipulator with freedom of movement, either rotationally or translationally (linearly). Any geometric axis about which a joint can rotate or extend along is counted as a single degree of freedom. Theoretically, there are many types of joints that provide different degrees of freedom in terms of rotation and translation, but in practice, most robotic arms will consist of joints that provide one degree of freedom. The two most famous joints used are:

- Swivel joint: Provides a degree of freedom of rotation
- Prismatic joint: Provides a linear degree of freedom

Robotic arms are often presented based on the total number of DoFs they have (Arsenault and Gosselin, 2006; Bandyopadhyay and Ghosal, 2003; Pennestri *et al*., 2005). Sometimes a "degree of freedom" is co-opted to be used for a function that does not result in "freedom". In other words, it doesn't move the position or orientation of the gripper/gripper/tool/sensor (the part of the robot that "does stuff"). On reach robotics manipulators, we typically have a set of jaws at the end of the robotic arm. To open or close the jaws of the robotic arm, a prismatic actuator (which only works along one axis) is used.

As the manipulator moves, this location is updated with respect to the "position" of the final effect. If it is desired to consider the position (x, y, z) with orientation (a, b, c), this position is optimized in the inverse kinematics algorithm (the most used). It was therefore considered that moving the linear actuator to open and close the grip of the manipulator does not change the reference point and therefore does not provide a "degree of freedom".

In this scenario, the prismatic actuator provides a "function" but not a "degree of freedom". As such, we can define a manipulator as having a different number of DoFs and Functions; for example, the Bravo 7 is a 7-function, 6-DoF manipulator, with one function being the opening/closing of the jaws (Fig. 1).

Why is all this important? One of the main things people are interested in when solving a complex robotic manipulator problem is DoF and its functions. These two distinct terminologies help keep conversations short and ensure everyone is on the same page!

It is no longer necessary to talk about the importance of industrial robots, considering that they recently reached the figure of three million industrial robots installed all over the planet, even if almost two-thirds of them work in Asia alone. The benefits they bring are already known, the fact that they have taken on heavy, tiring, repetitive work in dangerous environments and that they can work non-stop, at high speeds and with very good quality, at very low costs.

Today, however, dynamics cover a multitude of aspects, starting from forces in systems and going to new technologies and technological processes. A methodology for the flexible implementation of collaborative robots in intelligent manufacturing systems is presented in the paper (Giberti *et al*., 2022). A robot arm design optimization method using a kinematic redundancy resolution technique is presented in (Maaroof *et al*., 2021). Trajectory control of industrial robots using multilayer neural networks driven by iterative learning control can be found in the paper (Chen and Wen, 2021).

Dynamic and friction parameters of an industrial robot with repeatability identification, comparison, and analysis are other important aspects of dynamic and robotic processes in the industry (Hao *et al*., 2021). The impact of gravity compensation on reinforcement learning in goal-setting tasks for robotic manipulators is a relatively new problem in dynamic disciplines (Fugal *et al*., 2021). Another dynamic new aspect is the mechatronic redesign of a manual assembly workstation in collaboration with wiring assemblies (Palomba *et al*., 2021), which can be directly associated with new technological processes.

Another aspect of the dynamic process appears in (Yamakawa *et al*., 2021) through the development of a high-speed, low-latency, remote-controlled robotic manual system. Accessible educational resources for teaching and learning robotics (Pozzi *et al*., 2021) is also a dynamic aspect, but different from the physical-mechanical one that is of particular interest to us in this study.

Fig. 1: A 4 DoF and a 6 DoF robot; Source: https://reachrobotics.com/media/Article-Imagery-Infographic-01-2-1536x864.jpg

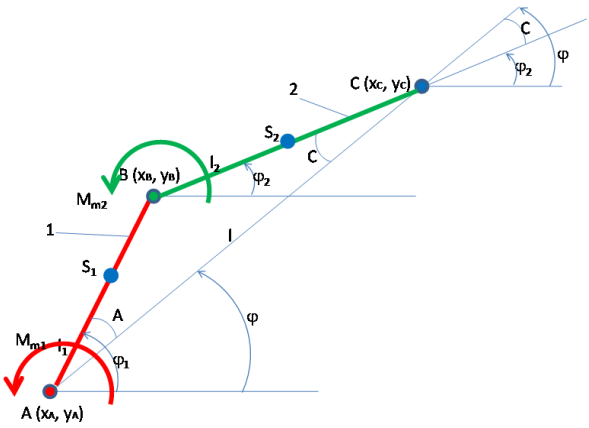

Fig. 2: A basic DoF robot

Dynamic identification of the parameters of a pointing mechanism taking into account joint play (Sun *et al*., 2021) is a basic dynamic process. The impact of cycle time and payload of an industrial robot on resource efficiency (Stuhlenmiller *et al*., 2021) is also an important aspect of dynamic processes. Today, adaptive position (or force) control of a robot manipulator (Gierlak, 2021; Geng *et al*., 2021), as well as trajectory control (Colan *et al*., 2021; Liu *et al*., 2021; Engelbrecht *et al*., 2021; Alizade *et al*., 2021; Scalera *et al*., 2021; Oliveira, 2013; Harrison and Nettleton, 1997; Besdo, 1973; Petrescu, 2012; 2014; 2022), are important dynamic processes.

Another important dynamic aspect (Essomba, 2021; Miguel-Tomé, 2021) is the balancing of technological processes (Caruso *et al*., 2021; Ebel *et al*., 2021; Thompson *et al*., 2021; Vatsal and Hoffman, 2021; Al Younes and Barczyk, 2021; Pacheco-Gutierrez *et al*., 2021; Stodola *et al*., 2021; Raviola *et al*., 2021; Medina and Hacohen, 2021; Malik *et al*., 2021).

The current work starts from the basic structure of the DoF robots, consisting of two mobile elements linked together by a kinematic rotation coupler, each of the two mobile elements (denoted in the work with 1 and 2 respectively, or the left and right element) being actuated by a rotary actuator (Fig. 2).

Rotary motors actuate the mobile elements 1 and 2, in *A* and *B*. *AB* = *l*1, *BC*=*l*2 is the length of the mobile elements 1 and 2, and j_1 (or f_1) and j_2, (or f_2), are the angles that position the mobile elements in relation to the Ox axis. The mass of mobile element 1 is considered concentrated in the center of symmetry *S*1, while the mass of mobile element 2 will be concentrated in the center of symmetry *S*2 (Petrescu and Petrescu, 2016; 2021; Petrescu, 2012; 2014; 2022).

One may have a robot (or several, possibly a robotic cell) and we want to know more about the components and user-replaceable parts, or perhaps we want to know more about how major robot assembly's work.

User-replaceable components of most robots include the end effector, sensors, and robot controller. For mobile robots, batteries will need to be replaced periodically. Important accessories for robots are the support of a robot arm and mounting systems for attaching sensors. The robot's vision system can also be replaceable. There are, of course, many other parts and smaller parts, such as LED displays and keyboards. We do not want to present here a complete list of all the component parts but only a small basic guide to the major assemblies and their functions:

- Robot end effectors
- Robot sensors
- Robot controllers
- Robot batteries
- Robot base/mounting systems
- Safety components for the robot
- Conveyor belts
- Vibrating feeders

The end effector of a robotic arm is where the actual work takes place. This is where the contact between the robot and the workpiece takes place. As with human beings, who use a very wide range of tools to get things done, so is with robots.

Robotic end effectors are also called "End of Arm Instruments" or EoATs. The EoAT is actually the robot's wrist, hand, and tool. End effectors can be anything from welding, machining, painting, cutting, and conveying tool, to a vacuum cleaner.

The EoAT could be a screwdriver or a rotary drill. Some companies specialize in making nothing but robotic end-effectors. Many providers only focus on certain types of EoAT.

It's often a nice feature to be able to switch tools automatically. A special device holds the tools. It is usually mounted on a surface external to the robot. The device can hold a variety of tools that the robot arm can swap in and out. In this way, the robot can perform different tasks on a workpiece. Here is an example of how this feature can be used: A robotic arm can drill a hole in a piece of metal. Then he changes tools and deburrs the hole he just made. The robot changes gears again. And use a tool to cut thread in the hole.

There are many different grippers available for robotic arms. A universal grip has not yet been found. At first, designers thought the best approach would be to create a grasping robot that was like a human hand. Later, they began to change their optics.

If the robot has to lift boxes all day, does it have to have fingers on its hand just like a human? Probably not. Humans do get tired of repetitively lifting various objects and fatigue is even greater and sets in faster if a human will repeatedly lift the same type of object without breaks. The human hand is designed to perform many types of operations, so it is not a good model for a gripper specialized in certain types of repetitive operations. For example, for smaller boxes, a suction cup might be even better. For larger boxes, it might be better to have a two-arm robot. The "hands" or clamps could be shaped like a sphere with knobs on them. For large and heavy boxes, it would be best to have a clamp that slides under the box and supports it from below.

As with many things in life, "form follows function." The type of gripper we need, or set of grippers, will depend on the respective major application that the robot in question will be using.

Robot sensors are like human senses. Robots can see, hear and have a sense of touch. They can be provided today even with the sense of smell and taste and they will not be lost even if the robot contracts COVID because it will not be affected by the disease at all. Industrial robots could use their sense of "smell" to test air quality in a mine. It could detect noxious gases or contaminant leaks. There are also tasting bots. They can test the quality of food and detect the presence of harmful chemicals. But the most common robotic sense currently used for industrial applications is vision. For this reason, let's take a brief look at some of the main types of sensors for robotic vision.

Optical Sensors

The variety of optical sensors now available for robots is truly impressive. Some sensors use optical methods to determine the roughness of a surface. Others can measure the thickness of a film. Others discover the exact color of objects. A robot can be equipped with a microscope. This opens up a world of possibilities. Many measurements can be made with a robotic microscope.

Optical sensors can measure the flow rate of a liquid. Flow can also be measured in other ways, such as with electromagnetic sensors. A kind of paddle wheel that sends pulses can also be used. The pulses appear faster when the wheel spins faster. Position and speed can also be measured with optical sensors. The sensors don't have to be video cameras, they are built specifically for robotic vision like human eyes, but today they can far exceed human visual capabilities because they can see like a microscope and in the future even an electronic one or more special so that the robot to see objects of nano (10^{-9}) or maybe even pico (10^{-12}) size, while the human eye can hardly see at most an object of a tenth of a millimeter (10^{-4}) size.

Robots can have binocular or telescopic eyes that bring objects at great or even astronomical distances closer, while the human eye cannot see clearly more than 100 m.

With the help of lasers, robots can read absolutely anything extremely quickly at any small or large distance, but with infrared rays, they can also do this at night in total darkness.

Laser Scanners

The introduction of laser technology into industrial applications has changed the way many things are done. Lasers are used in handheld barcode scanners. They can make accurate measurements of machined parts. Lasers are also used to measure long distances. Complex vision systems use lasers. Computer vision means mobile robots can navigate their way autonomously, avoiding obstacles in their path.

Visual lasers were very expensive at the beginning, but as time went by, they continuously became cheaper, becoming attractive from an economic-financial point of view.

Laser scanners for reading barcode labels are fast, accurate, and low-cost. Some scanners are portable and used by people in inventory management. Handheld laser scanners are also used in material handling and manufacturing tasks. Laser barcode scanners can be installed on Autonomous Mobile Robots (AMR) in warehouses to assist in the order-picking process. Scanners can be mounted on aerial drones that fly through warehouse aisles. Drones read barcodes and use computer vision to count items in boxes. Aerial drones can take inventory in a fraction of the time it takes humans to do so.

Laser barcode scanners aren't the only way to keep track of items. RFID-based scanners could be used. Radio Frequency Identification (RFID) has the advantage that the tag does not have to be visible and can still be read. This is because RFID uses radio waves instead of light. But RFID tags are more expensive today than barcodes, they can be read even when they are embedded inside an object or a box.

One of the most common uses for laser scanners is industrial robotics vision. These scanners use LiDAR, which stands for Light Detection and Ranging. LiDAR is like RADAR. Radar was invented during World War II and stands for radio detection and ranging. In both cases, the principle is similar. The LiDAR sensor sends out a pulse of electromagnetic energy and then detects the reflection coming from the nearest object in its path. The time required for the reflections to return is measured. If it takes longer for the reflection to return, the object is further away. A shorter time means the object is closer. The time is proportional to the distance from the sensor to the object. In this way, lasers can be used to accurately measure the distance to a single point.

Today, robotic sensor radars precisely measure a certain landmark location, against which the robot can position itself and even balance permanently, a fact extremely useful in aerospace, aircraft, and drones.

Fun fact: NASA scientists invented LiDAR in the 1960s as part of the Apollo moonshot program. One of its first uses was to measure the distance between the Earth and the Moon.

LiDAR today can be used in one 1-D, two 2-D, and three 3-D dimensions. An example of LiDAR in one dimension is a laser tape measure. You can quickly and accurately measure the dimensions of a room or a building with it. For industrial applications, lasers are used to precisely measure the depth of a cut made by a machine tool or robotic milling machine. Robot arms with LiDAR can measure the size of a part for quality control.

In a 2-D setup, a laser beam is scanned back and forth. The scan can go in a full circle or only pass through part of the circle. The laser beam remains in a two-dimensional plane. For an Autonomous Mobile Robot (AMR), this plane is horizontal. It is often several inches above the ground. In this way, AMR can use its LiDAR to detect objects in its path. The robot uses this awareness to determine if it is safe to continue on the planned route. If something blocks its path, the robot can slow down, stop, or adapt to perform a detour by changing direction.

But 2-D LiDAR has the limitation that it cannot detect objects above or below the laser scan plane. In effect, the robot is "blind" to anything not in the plane of the 2-D LiDAR. Using 3-D LiDAR can overcome this limitation successfully, at a slightly higher price.

With 3-D LiDAR, the system scans the laser beam in a plane (like 2-D LiDAR), and then the object (plane) is tilted up and down. The addition of the tilting action means that the system spans a three-dimensional space. The downside of 3-D scanning is that it requires more computing power. The system gathers a lot more information, so it's a challenge to process all that information and do it in real time. This requires more powerful computers. Also, the mechanical components of 3-D LiDAR are more complex. Therefore, 3-D scanners are more expensive than 2-D scanners. It all depends on the application, whether 2-D or 3-D scanning is appropriate.

Of course, there are limitations to LiDAR. Direct sunlight can blind a LiDAR sensor. However, LiDAR can handle more intense sunlight than many types of sensors. The object reflecting the laser beam can damage things. The type of material and color of reflective objects can affect LiDAR accuracy. Dust, dirt, and debris can clog the lens of a LiDAR sensor. This will reduce the sensitivity and accuracy of the sensor.

To overcome this impediment, it is necessary to switch from lasers to electromagnetic waves.

Vision Systems

Robot vision has undergone revolutionary changes. Not long ago, robot vision was very limited. So limited, in fact, that if a robot detected something in the way, all it could do was stop and call for help. Today, autonomous mobile robots can avoid obstacles in their path. They can tell the difference between people and inanimate objects.

The resolution and sensitivity of the cameras have increased. The software that processes the visual data has also improved. Computer vision systems now recognize human faces.

Camera hardware is an important part of the vision solution. But recording raw data is not enough. The vision system must be able to transform that data into useful information. The vision system must be able to detect the distance, speed, and direction of an object. It is even more useful if the vision system can recognize that an object is a person or a forklift. The ability to understand that one object is a person while another is a vehicle is called semantics. Semantic understanding of an environment is crucial to making robots smarter.

Another use of computer vision is order picking. The robot must be able to pick an object, even when the object is in a pile of other things. This is called picking out of disorder. The robot must identify not only the object, but also whether it is lying normally, tilted, or upside down. Once this is determined, the robot can decide how to pick up the object. This has proven to be a challenge, but now there are systems that can do this in an easy way.

Robotic Vision Through Sensor Fusion

Increasingly, robotic systems rely on a combination of sensors. Each of the different sensor types has strengths and weaknesses. Even a single sensor can provide some kind of "vision" for a robotic system. But a combination of sensors is the best choice. Combining data from multiple sensors is called sensor fusion. In this way, we use two or even more eyes, placed in different positions and the vision of the robot is much better after the different images obtained from all eyes are compiled by a microprocessor and merged to generate a unique (overall)

image. Sensor fusion makes a robot more robust, reliable, and safe. As the computing power of microchips continues to grow, we can expect to see more and more sensors (eyes) being used. This will make robots even smarter and more capable.

For example, we could have two or more eyes for normal vision, another pair for long-distance vision (several km), another pair for seeing at astronomical distances, another pair for microscopic vision, one for all-seeing absolute darkness, another to penetrate through objects and materials to visualize the elements located inside objects or beings and even more eyes destined for a perfect overview. Such a multi-visual robotic system will have special capabilities, being stronger than any current being, starting the cycle of development of multi-capable and ultra-intelligent robots of the future.

Robot Controllers

The brains of the robot, the controllers, are also as important as its eyes, far surpassing in importance the actuators (which are also closely related to the thinking system, acting being possible only together with adequate thinking both in robots and in people, but also with a good vision system that tells the robot when to act and when not). Robot controllers come in a variety of shapes and sizes. Some are small, portable tablets. These are used to control a simple work cell. Other robot controllers can control complex manufacturing and logistics processes. The robot controller is crucial to determining how easy it is to get a robotic system to do what you want. The robot controller is a critical part of how the robot performs its work.

Robot controllers are responsible for safety, logic, and motion control. How quickly a robot responds to an external event is often a critical metric for a robot controller. Some applications need a faster response time than others. This can determine the type of robot controller needed. The Human-Machine Interface (HMI) of a robot controller is another important aspect. A popular HMI is a "teaching pendant" which is a portable, tablet-type device. The teach pendant is used when teaching the robot what to do. Once the robot is ready for production, the teach pendant can be removed.

In a factory, it is more common to find a wired connection between a robot controller and the robot. The wired connection provides a reliable and secure interface. Safety regulations sometimes require a wired connection (or both) (even if a wireless one is also available). This does not apply to Autonomous Mobile Robots (AMR). An AMR wouldn't be much use if it had to have a wire attached to the controller! Wireless industrial robot controllers are also available. Depending on the application, they may have advantages over wired systems. Otherwise, the controller is built-in for independent autonomous robots, but they can also have an external wireless control controller that can do manual control or when the autonomous robot needs corrections from the base.

There are three broad categories of robotic controllers:

- PLC (Programmable Logic Controller)
- PAC (Programmable Automation Controller)
- IPC (Industrial Personal Computer)

PLC is the oldest technology and the lowest-cost type of robot controller. It is used for simple applications that do not require complex motion control. A PLC's data logging capability is also less capable than other types of robot controllers. The PLC will have fewer types of input/output devices. Simple, small, cheap, and effective for small and or less sophisticated systems.

PAC is an updated version of PLC. PAC has more computing power and greater capacity. There is a very wide range of applications for which a PAC is suitable.

IPC has the most computing power and is also the most expensive type of robot controller. It can handle complex movements and communicate through a wide variety of interfaces. IPC can handle and store very large amounts of data.

The distinctions between these three types of controllers become more blurred over time. Today, there really aren't three separate categories of robot controllers anymore. There is more of a continuum.

When choosing between different robot controllers, an important factor is the software. It's good to look for application-specific software packages. The application package will determine how easy it is to get that robotic system up and running. It will also influence how much support you can expect for your particular needs from that bot:

- The robot's power system
- Powering a robot is a very serious matter
- The evolution of battery technology has affected a wide range of electrical and electronic devices

Better batteries mean longer operating times (increased autonomy) and shorter charging intervals. Improvements have made Autonomous Mobile Robots (AMRs) practical and cost-effective.

Some of the basic things to consider when choosing the right robot battery for the application include chemistry, capacity, and charging.

The chemical composition of a robot battery will generally be of the following types.

NiMh: Nickel-metal hydride batteries are still the most common type of battery used for robots. They are good value due to the weight/capacity ratio and there is very little 'memory effect'. Memory effect is a limitation of certain types of batteries. It means that the battery must be fully discharged before recharging. Otherwise, part of the battery's capacity is lost each time it is recharged.

NiCd (Nickel Cadmium) batteries suffer from the memory effect and are being replaced today by other types of batteries.

Classic lead-acid batteries still offer high capacity and low cost. Despite the pollution from lead and acid and their higher mass, these batteries are still used in robots, vehicles, and autonomous robots.

LiPo (Lithium-ion Polymer) batteries are often simply called "lithium batteries". They are fast becoming the battery of choice for robots due to their high capacity/weight ratio. In addition, it does not suffer from the memory effect. Their only problem today is the increasing use of lithium for accumulators and batteries of all kinds, in the nuclear industry, the medical industry, etc., so that lithium becomes an increasingly precious and sought-after material, still difficult to replace with another.

Questions to ask when considering battery choice include: How long does it take to charge the battery? Does the battery charger have overcharge protection? Wireless charging can also be quite useful for robots. Charging is easier because the robot does not need to be in a precise position when it arrives at the charging station. Another basic question is the autonomy offered by that battery. The lifespan and the purchase price are also taken into account.

Stationary robots with robotic arms must be securely mounted to perform their tasks. There are many options from which to choose the most suitable system.

Pedestal support is useful when we need to have a raised robot arm. The boom may need to be raised to access conveyor systems and work surfaces. The supports can be fixed to the floor. The stands can also have wheels so they can be moved around easily.

There are applications for which it is ideal to have a robot mounted in an inverted position. There are special supports for this. An inverted orientation can often maximize the reach of the arm. Other applications may require the robot to be mounted vertically. It can be fixed on the side of a car. Once the position is determined, the software that comes with the robot arm will need to be adjusted.

Modular mounting systems are available for fixing the sensors. Examples include cameras, cables, and hoses. Some sensor mounting systems are best for their strength and durability. Other times the emphasis is on flexibility and lightweight for portability. Adjustable levers allow the correct positioning of sensors and cables.

Materials and Methods

A classic 2 DoF robot has two mobile elements (1 and 2) connected to each other by an internal coupling B and two semi-couples (potential couplings) A and C, which are also connected to other possible elements. In general, coupler A attaches to a pivoting column that supports the entire robot like a spine and rotates it in space. Couple C is connected either to the final effector element or to another arm (or to an additional structure) that can increase the structure of the entire robot (in which case it increases its degrees of freedom from 3 to 4, 5, or even 6). The basic articulated robot under discussion is one consisting of a vertical pivoting column and two articulated arms attached to it, which have a planar movement. To simplify the study, only the flat part of the robot will be considered, without the pivoting vertical column, that is, only the forearm (element 1) and arm (element 2) of the 3 DoF articulated robot will be studied (Fig. 3). Mobile element 1 is driven by an actuator positioned in joint A (coupling between the pivoting column that supports the robot and the mobile forearm marked with 1). The length of element *1* is $l_1 = AB$ and its mass m_1 is considered to be concentrated in the center of symmetry S_1 located at the distance $ls_1 = AS_1$ from the movable joint A. Mobile element 2 is driven by an actuator positioned in joint B (coupling between the mobile forearm 1 and the mobile arm marked with 2). The length of element 2 is $l_2 = BC$ and its mass m_2 is considered to be concentrated in the center of symmetry S_2 located at the distance $ls_2 = BS_2$ from the movable joint B. The absolute positioning angles of the two mobile elements 1 and 2, respectively, are denoted ϕ with respect to the horizontal axis or θ with respect to the vertical axis. In the framework of the works, the horizontal axes parallel to the abscissa axis of the main Cartesian system of axes will be used for positioning, which for simplicity was considered in this case with the origin in couple A. One will thus have a first generalized coordinate by the ϕ_1 angle (measured in radians) that absolutely positions element 1 in relation to the horizontal axis that passes through coupling *A* and a second generalized coordinate ϕ_2 (measured in radians) that absolutely positions element 2 in relation to the horizontal axis that passes through coupling B.

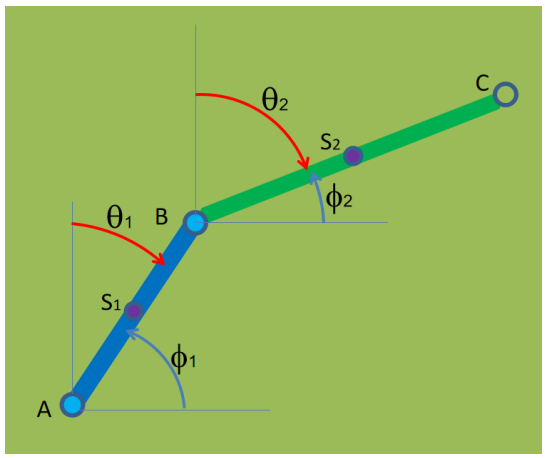

Fig. 3: The basic planar system of a 2 DoF robot

Some specialists prefer to consider the vertical axis as the absolute positioning axis, in which case the generalized coordinate θ_1 (measured in radians) will be used for the positioning of mobile element 1 $(\theta_1 = \phi_1 - \pi/2)$ and the second generalized coordinate θ_2 for the absolute positioning of mobile element 2 $(\theta_2 = \phi_1 - \pi/2)$. The end effector of the robot is attached to the C coupling. All the units of measure used are those indicated by the international standard so that no confusion arises or transformations of the units of measure are necessary. All lengths are considered in meters; l_1=*AB* represents the length of mobile element 1 and AS_1= ls_1 is the distance from coupling A to the center of symmetry S_1 of element 1. Similarly, the length of mobile element 2 is defined *as* l_2 = *BC* and the distance from coupling *B* to the center of symmetry S_2 of element 2 is $BS_2 = ls_2$. The masses of the two elements are taken in kg, m_1 representing the mass of mobile element 1, considered to be concentrated in the center of symmetry S_1, and m_2 representing the mass of element 2, considered to be concentrated in the center of symmetry S_2.

Lagrange II Dynamics Method

The dynamics of the 2 DoF robot will initially be studied using the Lagrange type II method. The great advantage of the Lagrange method is that it does not need to determine exactly all the forces acting in the system because their effect will be studied through the total linear energies of the system. For this reason, the accelerations of the centers of symmetry (of mass) of the system are not necessary, but only their velocities. In fact, Lagrange is the first scientist who introduced the use of the total energies of a machine to determine its dynamics (Oliveira, 2013; Harrison and Nettleton, 1997). Later, the energy methods were also used by Hamilton and many other scientists. Determining the real motion of a 2 DoF robot can be done most correctly with the help of the forces acting on the respective robot because they are the ones that determine the real motion.

The attempt to use energy methods instead of forces is due to Lagrange and it will further describe his method of the second type applied in the case of the present work to a 2 DoF robot. The starting equations for the Lagrange total energy method are the two of the translational kinetic energy of the robot mechanism, denoted by *T*, and that of its potential energy, denoted by *V* (Harrison and Nettleton, 1997; Besdo, 1973). Both equations were described within the relational system (1) (Harrison and Nettleton, 1997; Besdo, 1973). As a novelty brought by the author of the work, there is an additional concentrated mass m_C (measured in kilograms) introduced at point C by the weight force (technological resistance, R_T) that presses on element 2, in the coupling *C*. Traditionally, technological resistance is treated only by the method of forces because it is an additional force in the system, practically an additional force of gravity. Since its effect is more important than the one given by the respective weight force, one considered the fact that this force (additional weight, technological resistance, R_T; Fig. 4) introduces a concentrated mass (additional, $m_C = R_T/g$) into the system, which behaves similarly to concentrated masses m_1 and m_2, having kinetic energy (in the Lagrange method) or generating inertial forces (in the force method). All forces are considered in *N* and moments in Nm. Linear speeds are measured in meters/second and angular speeds are in hertz = s^{-1}. Linear accelerations are measured in meters per second squared and angular ones in Hertz squared (s^{-2}). The torsor of inertial forces is composed of the inertial forces acting on the mobile element 1, concentrated in the center of symmetry S_1, with a horizontal component $F_{S_1}^{ix}$ and a vertical one $F_{S_1}^{iy}$, plus a moment M_1^i and of the inertial forces acting on the mobile element 2, concentrated in the center of symmetry S_2, with a horizontal component $F_{S_2}^{ix}$ and a vertical one $F_{S_2}^{iy}$, plus a moment M_2^i. It also presents two weights G_1 and G_2 respectively and the technological resistance R_T that acts at point *C* similar to a force of gravity. The scalar components of the linear velocities for the two centers of symmetry S_1 and S_2, respectively, are $\dot{x}_{S_1}$ $\dot{x}_{S_2}$ on the horizontal axes and $\dot{y}_{S_1}$ $\dot{y}_{S_2}$ respectively on the vertical axes. Similarly, the two scalar speeds $\dot{x}_C$ $\dot{y}_C$ are defined at point *C*. The scalar coordinates of the vertical axes are y_{s1}, y_{s2}, and y_C and *g* represents the gravitational acceleration:

$$\begin{cases} T = \frac{1}{2} m_1 \cdot \left(\dot{x}_{S_1}^2 + \dot{y}_{S_1}^2\right) + \frac{1}{2} m_2 \cdot \left(\dot{x}_{S_2}^2 + \dot{y}_{S_2}^2\right) + \frac{1}{2} m_C \cdot \left(\dot{x}_C^2 + \dot{y}_C^2\right) \\ V = m_1 \cdot g \cdot y_{S_1} + m_2 \cdot g \cdot y_{S_2} + m_C \cdot g \cdot y_C \end{cases} \quad (1)$$

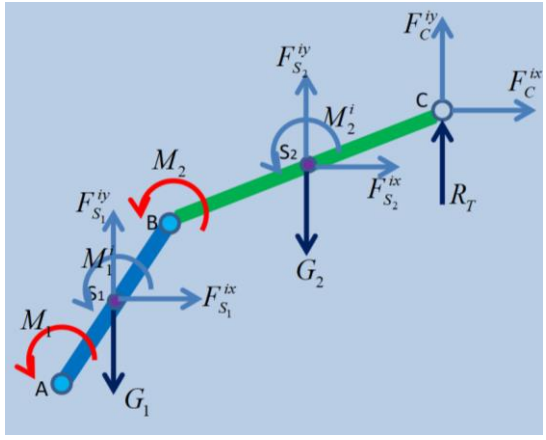

Fig. 4: The forces acting in a basic planar system of a 2 DoF robot

Next, the relational system (2) of positions and velocities is written with the help of which Eq. (1) of kinetic energy T and potential energy *V* acquire the developed form (3). Here one can see the first advantage of the Lagrange method, namely the fact that it is necessary to write only the parametric equations of positions and velocities, unlike the method of forces where the velocities must be derived and the acceleration equations are also needed; ω_1 represents the angular speed of mobile element 1 and ω_2 is the angular speed of mobile element 2, both being measured in hertz:

$$\begin{cases} \begin{cases} x_{S_1} = ls_1 \cdot \cos\phi_1 \\ y_{S_1} = ls_1 \cdot \sin\phi_1 \end{cases} \begin{cases} \dot{x}_{S_1} = -ls_1 \cdot \sin\phi_1 \cdot \omega_1 \\ \dot{y}_{S_1} = ls_1 \cdot \cos\phi_1 \cdot \omega_1 \end{cases} \\ \begin{cases} x_{S_2} = l_1 \cdot \cos\phi_1 + ls_2 \cdot \cos\phi_2 \\ y_{S_2} = l_1 \cdot \sin\phi_1 + ls_2 \cdot \sin\phi_2 \end{cases} \begin{cases} \dot{x}_{S_2} = -l_1 \cdot \sin\phi_1 \cdot \omega_1 - ls_2 \cdot \sin\phi_2 \cdot \omega_2 \\ \dot{y}_{S_2} = l_1 \cdot \cos\phi_1 \cdot \omega_1 + ls_2 \cdot \cos\phi_2 \cdot \omega_2 \end{cases} \\ \begin{cases} x_C = l_1 \cdot \cos\phi_1 + l_2 \cdot \cos\phi_2 \\ y_C = l_1 \cdot \sin\phi_1 + l_2 \cdot \sin\phi_2 \end{cases} \begin{cases} \dot{x}_C = -l_1 \cdot \sin\phi_1 \cdot \omega_1 - l_2 \cdot \sin\phi_2 \cdot \omega_2 \\ \dot{y}_C = l_1 \cdot \cos\phi_1 \cdot \omega_1 + l_2 \cdot \cos\phi_2 \cdot \omega_2 \end{cases} \end{cases} \tag{2}$$

$$\begin{cases} T = \frac{1}{2} m_1 \cdot ls_1^2 \cdot \omega_1^2 + \frac{1}{2} m_2 \cdot \left[l_1^2 \cdot \omega_1^2 + ls_2^2 \cdot \omega_2^2 + 2 l_1 \cdot ls_2 \cdot \cos(\phi_1 - \phi_2) \cdot \omega_1 \cdot \omega_2 \right] + \\ \frac{1}{2} m_C \cdot \left[l_1^2 \cdot \omega_1^2 + l_2^2 \cdot \omega_2^2 + 2 l_1 \cdot l_2 \cdot \cos(\phi_1 - \phi_2) \cdot \omega_1 \cdot \omega_2 \right] \\ V = (m_1 \cdot ls_1 + m_2 \cdot l_1 + m_C \cdot l_1) \cdot g \cdot \sin\phi_1 + (m_2 \cdot ls_2 + m_C \cdot l_2) \cdot g \cdot \sin\phi_2 \end{cases} \tag{3}$$

One can now introduce the Lagrange Eq. (4) of the second type (Petrescu, 2012):

$$\begin{cases} \frac{d}{dt}\left(\frac{\partial T}{\partial \omega_1}\right) + \frac{\partial V}{\partial \varphi_1} = \frac{d}{dt}\left(\frac{\partial V}{\partial \omega_1}\right) + \frac{\partial T}{\partial \phi_1} \\ \frac{d}{dt}\left(\frac{\partial T}{\partial \omega_2}\right) + \frac{\partial V}{\partial \phi_2} = \frac{d}{dt}\left(\frac{\partial V}{\partial \omega_2}\right) + \frac{\partial T}{\partial \phi_2} \end{cases} \tag{4}$$

Next (5, 6) the parameters of the two Eq. (4) are entered step by step:

$$\begin{cases} \frac{\partial T}{\partial \omega_1} = \left(m_1 \cdot ls_1^2 + m_2 \cdot l_1^2 + m_C \cdot l_1^2\right) \cdot \omega_1 + \left(m_2 \cdot ls_2 + m_C \cdot l_2\right) \cdot l_1 \cdot \cos(\phi_1 - \phi_2) \cdot \omega_2 \\ \frac{d}{dt}\left(\frac{\partial T}{\partial \omega_1}\right) = \left(m_1 \cdot ls_1^2 + m_2 \cdot l_1^2 + m_C \cdot l_1^2\right) \cdot \varepsilon_1 + \left(m_2 \cdot ls_2 + m_C \cdot l_2\right) \cdot l_1 \cdot \cos(\phi_1 - \phi_2) \cdot \varepsilon_2 + \\ \left(m_2 \cdot ls_2 + m_C \cdot l_2\right) \cdot l_1 \cdot \sin(\phi_1 - \phi_2) \cdot \omega_2 \cdot (\omega_2 - \omega_1) \\ \frac{\partial V}{\partial \varphi_1} = (m_1 \cdot ls_1 + m_2 \cdot l_1 + m_C \cdot l_1) \cdot g \cdot \cos\phi_1 \quad \frac{\partial V}{\partial \omega_1} = 0 \Rightarrow \frac{d}{dt}\left(\frac{\partial V}{\partial \omega_1}\right) = 0 \\ \frac{\partial T}{\partial \varphi_1} = -\left(m_2 \cdot ls_2 + m_C \cdot l_2\right) \cdot l_1 \cdot \omega_1 \cdot \omega_2 \cdot \sin(\phi_1 - \phi_2) \end{cases} \tag{5}$$

$$\begin{cases} \frac{\partial T}{\partial \omega_2} = \left(m_2 \cdot ls_2^2 + m_C \cdot l_2^2\right) \cdot \omega_2 + \left(m_2 \cdot ls_2 + m_C \cdot l_2\right) \cdot l_1 \cdot \cos(\phi_1 - \phi_2) \cdot \omega_1 \\ \frac{d}{dt}\left(\frac{\partial T}{\partial \omega_2}\right) = \left(m_2 \cdot ls_2^2 + m_C \cdot l_2^2\right) \cdot \varepsilon_2 + \left(m_2 \cdot ls_2 + m_C \cdot l_2\right) \cdot l_1 \cdot \cos(\phi_1 - \phi_2) \cdot \varepsilon_1 + \\ \left(m_2 \cdot ls_2 + m_C \cdot l_2\right) \cdot l_1 \cdot \sin(\phi_1 - \phi_2) \cdot \omega_1 \cdot (\omega_2 - \omega_1) \\ \frac{\partial V}{\partial \phi_2} = (m_2 \cdot ls_2 + m_C \cdot l_2) \cdot g \cdot \cos\phi_2 \quad \frac{\partial V}{\partial \omega_2} = 0 \Rightarrow \frac{d}{dt}\left(\frac{\partial V}{\partial \omega_2}\right) = 0 \\ \frac{\partial T}{\partial \phi_2} = \left(m_2 \cdot ls_2 + m_C \cdot l_2\right) \cdot l_1 \cdot \omega_1 \cdot \omega_2 \cdot \sin(\phi_1 - \phi_2) \end{cases} \tag{6}$$

The Lagrange equations of the second type (order; 4) can now be expressed in the form of a system of two equations with two unknowns ($\ddot{\varphi}_{1L}; \ddot{\varphi}_{2L}$) (7), which are solved by the system (8; Kramer method):

$$\begin{cases} \begin{cases} \lg_{11} = m_1 \cdot ls_1^2 + m_2 \cdot l_1^2 + m_C \cdot l_1^2 \\ \lg_{12} = (m_2 \cdot ls_2 + m_C \cdot l_2) \cdot l_1 \cdot \cos(\phi_1 - \phi_2) \\ \lg_{21} = (m_2 \cdot ls_2 + m_C \cdot l_2) \cdot l_1 \cdot \cos(\phi_1 - \phi_2) \\ \lg_{22} = m_2 \cdot ls_2^2 + m_C \cdot l_2^2 \\ \lg_1 = -(m_2 \cdot ls_2 + m_C \cdot l_2) \cdot l_1 \cdot \sin(\phi_1 - \phi_2) \cdot \omega_2^2 - (m_1 \cdot ls_1 + m_2 \cdot l_1 + m_C \cdot l_1) \cdot g \cdot \cos\phi_1 \\ \lg_2 = (m_2 \cdot ls_2 + m_C \cdot l_2) \cdot l_1 \cdot \sin(\phi_1 - \phi_2) \cdot \omega_1^2 - (m_2 \cdot ls_2 + m_C \cdot l_2) \cdot g \cdot \cos\phi_2 \end{cases} \\ \begin{cases} \lg_{11} \cdot \ddot{\phi}_{1L} + \lg_{12} \cdot \ddot{\phi}_{2L} = \lg_1 \\ \lg_{21} \cdot \ddot{\phi}_{1L} + \lg_{22} \cdot \ddot{\phi}_{2L} = \lg_2 \end{cases} \end{cases} \tag{7}$$

$$\begin{cases} \Delta = \lg_{11} \cdot \lg_{22} - \lg_{12} \cdot \lg_{21} \\ \Delta_1 = \lg_1 \cdot \lg_{22} - \lg_{12} \cdot \lg_2 \\ \Delta_2 = \lg_{11} \cdot \lg_2 - \lg_1 \cdot \lg_{21} \\ \ddot{\phi}_{1L} = \frac{\Delta_1}{\Delta}; \ddot{\phi}_{2L} = \frac{\Delta_2}{\Delta}; \Delta\dot{\phi}_{1L} = \frac{\ddot{\phi}_{1L} \cdot \Delta\phi_1}{\omega_1}; \Delta\dot{\phi}_{2L} = \frac{\ddot{\phi}_{2L} \cdot \Delta\phi_2}{\omega_2}; D_c = \sin^2(\phi_1 - \phi_2) \\ \dot{\phi}_{1L} = \omega_1 + \Delta\dot{\phi}_{1L}; \dot{\phi}_{2L} = \omega_2 + \Delta\dot{\phi}_{2L}; \omega_{1L} = \dot{\phi}_{1L} \cdot D_c; \omega_{2L} = \dot{\phi}_{2L} \cdot D_c \end{cases} \tag{8}$$

The calculation program and simulations can be found in the appendix and the obtained results are presented.

Forces Dynamics Method

The dynamics of the 2 DoF robot will also be studied using the Forces method. Determining the real motion of a 2 DoF robot can be done most correctly with the help of the forces acting on the respective robot because they are the ones that determine the real motion. Next, we will present the calculation method of the basic dynamic parameters of a 2 DoF robot (Fig. 4), by using a method that uses the conservation of the robot's forces on the axes of the x and y scalars (system of Eq. (9). Equations (9) are developed in the form (10) and by introducing the expressions of scalar accelerations (11), they take the form (12), i.e., a system of two linear equations with two unknowns $(\ddot{\phi}_1; \ddot{\phi}_2)$ which is solved by the system (13), Kramer method. The final dynamic angular velocities will be obtained by amplifying those resulting from the system of forces with the dynamic coefficient D_c of the internal coupling of the system, which also introduces the dynamic coupling effect.

$$\begin{cases} \sum F_x^{(1,2)} = 0 \Rightarrow F_{S_1}^{ix} + F_{S_2}^{ix*} + F_C^{ix} = 0 \\ \sum F_y^{(1,2)} = 0 \Rightarrow F_{S_1}^{iy} + F_{S_2}^{iy*} + F_C^{iy} = 0 \end{cases} \tag{9}$$

$$\begin{cases} -m_1 \cdot \ddot{x}_{S_1} - m_2 \cdot \ddot{x}_{S_2} - m_C \cdot \ddot{x}_C = 0 \\ -m_1 \cdot (\ddot{y}_{S_1} + g) - m_2 \cdot (\ddot{y}_{S_2} + g) - m_C \cdot (\ddot{y}_C + g) = 0 \end{cases} \tag{10}$$

$$\begin{cases} \ddot{x}_{S_1} = -ls_1 \cdot \ddot{\phi}_1 \cdot \sin\phi_1 - ls_1 \cdot \dot{\phi}_1^2 \cdot \cos\phi_1 \\ \ddot{y}_{S_1} = ls_1 \cdot \ddot{\phi}_1 \cdot \cos\phi_1 - ls_1 \cdot \dot{\phi}_1^2 \cdot \sin\phi_1 \\ \ddot{x}_{S_2} = -l_1 \cdot \ddot{\phi}_1 \cdot \sin\phi_1 - l_1 \cdot \dot{\phi}_1^2 \cdot \cos\phi_1 - ls_2 \cdot \ddot{\phi}_2 \cdot \sin\phi_2 - ls_2 \cdot \dot{\phi}_2^2 \cdot \cos\phi_2 \\ \ddot{y}_{S_2} = l_1 \cdot \ddot{\phi}_1 \cdot \cos\phi_1 - l_1 \cdot \dot{\phi}_1^2 \cdot \sin\phi_1 + ls_2 \cdot \ddot{\phi}_2 \cdot \cos\phi_2 - ls_2 \cdot \dot{\phi}_2^2 \cdot \sin\phi_2 \\ \ddot{x}_C = -l_1 \cdot \ddot{\phi}_1 \cdot \sin\phi_1 - l_1 \cdot \dot{\phi}_1^2 \cdot \cos\phi_1 - l_2 \cdot \ddot{\phi}_2 \cdot \sin\phi_2 - l_2 \cdot \dot{\phi}_2^2 \cdot \cos\phi_2 \\ \ddot{y}_C = l_1 \cdot \ddot{\phi}_1 \cdot \cos\phi_1 - l_1 \cdot \dot{\phi}_1^2 \cdot \sin\phi_1 + l_2 \cdot \ddot{\phi}_2 \cdot \cos\phi_2 - l_2 \cdot \dot{\phi}_2^2 \cdot \sin\varphi_2 \end{cases} \tag{11}$$

$$\begin{cases} f_{11} = (m_1 \cdot ls_1 + m_2 \cdot l_1 + m_C \cdot l_1) \cdot \sin\phi_1 \\ f_{12} = (m_2 \cdot ls_2 + m_C \cdot l_2) \cdot \sin\phi_2 \\ f_{21} = (m_1 \cdot ls_1 + m_2 \cdot l_1 + m_C \cdot l_1) \cdot \cos\phi_1 \\ f_{22} = (m_2 \cdot ls_2 + m_C \cdot l_2) \cdot \cos\phi_2 \\ f_1 = -f_{21} \cdot \dot{\phi}_1^2 - f_{22} \cdot \dot{\phi}_2^2 \\ f_2 = f_{11} \cdot \dot{\phi}_1^2 + f_{12} \cdot \dot{\phi}_2^2 - g \cdot (m_1 + m_2 + m_C) \\ f_{11} \cdot \ddot{\phi}_1 + f_{12} \cdot \ddot{\phi}_2 = f_1 \\ f_{21} \cdot \ddot{\phi}_1 + f_{22} \cdot \ddot{\varphi}_2 = f_2 \end{cases} \tag{12}$$

$$\begin{cases} \Delta_f = f_{11} \cdot f_{22} - f_{12} \cdot f_{21} \\ \Delta_{f1} = f_1 \cdot f_{22} - f_{12} \cdot f_2 \\ \Delta_{f2} = f_{11} \cdot f_2 - f_1 \cdot f_{21} \\ \ddot{\phi}_1 = \frac{\Delta_{f1}}{\Delta_f}; \ddot{\phi}_2 = \frac{\Delta_{f2}}{\Delta_f}; \Delta\dot{\phi}_1 = \frac{\ddot{\phi}_1 \cdot \Delta\phi_1}{\dot{\varphi}_1}; \Delta\dot{\phi}_2 = \frac{\ddot{\phi}_2 \cdot \Delta\phi_2}{\dot{\phi}_2}; D_c = \sin^2(\phi_1 - \phi_2) \\ \dot{\phi}_{1D} = \dot{\phi}_1 + \Delta\dot{\phi}_1; \dot{\phi}_{2D} = \dot{\phi}_2 + \Delta\dot{\phi}_2; \omega_{1D} = \dot{\phi}_{1D} \cdot D_c; \omega_{2D} = \dot{\phi}_{2D} \cdot D_c \end{cases} \tag{13}$$

Results and Discussion

In the presented example, the masses, dimensions, and technological resistance from the appendix were considered. An independent variable k was considered, to be able to write the calculation program (see the appendix). In the inverse kinematics in which the 3 DoF robot is forced to work, its end-effector *C* is moved on a circle (Fig. 5). The scalar coordinate y_B and x_B are determined using an original algorithm (see the appendix). With an original simple algorithm, the positioning angles ϕ_1 and ϕ_2 (of the two mobile elements 1 and 2) are determined (see the appendix). The command, control, and automation of the speeds of the two mobile elements 1 and 2 are also done with a simple and original algorithm (see the appendix or (Petrescu, 2012; 2022)). It must be specified that in the simulation program in Mathcad, an independent variable k was considered, which has the advantage that it can then be expressed in terms of generalized coordinates or even time. In the considered example, the independent variable k (dimensionless) was forced to take values from 0 to 400.

Lagrange Ii Dynamics for A 3r Robot

The Lagrange II dynamics algorithm can be found in the appendix. Next, the results obtained with his help will be presented. The angular velocity ($\omega_{1,or2}$ in red) compared to that of Lagrange dynamics (ϕ_{11L} , or ϕ_{21L} in blue) will be presented both for mobile element 1 (robot forearm; Fig. 6) and for mobile element 2 (arm; Fig. 7). The vast majority of the parameters in the paper vary (including in the diagrams in the figures) depending on the independent and dimensionless variable denoted by k.

The angular velocity (ω_1 or ω_2 , in red) versus that of the Lagrange dynamics plus the dynamics imposed by the internal couple B (ω_{1L} or ω_{2L} , in blue) will be shown for both mobile element 1 (the robot's forearm; Fig. 8) and mobile element 2 (the arm; Fig. 9).

It can be seen (Figs 8-9) that the influence of the inner couple B is much greater than that of the external forces (obtained here with the help of Lagrange equations of the second order). In other words, the general dynamics is majorly influenced by the couple that connects the two elements in motion, and only in second place is the influence of the external forces that act on the robot (inertia forces, weights, technological resistances).

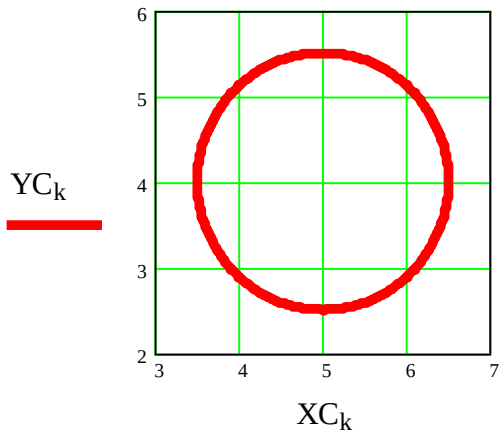

Fig. 5: In the inverse kinematics in which the 3 DoF robot is forced to work, its end-effector C is moved on a circle

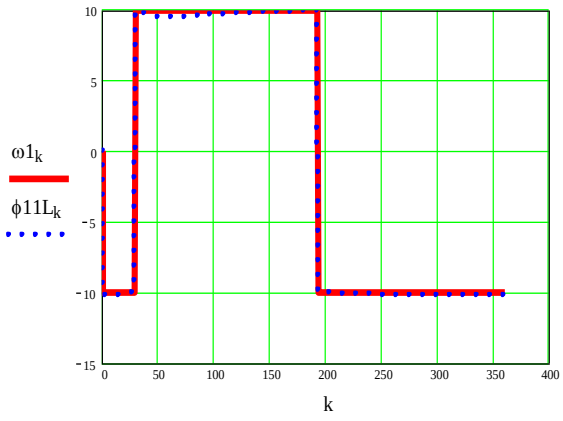

Fig. 6: The angular velocity (in red) compared to that of Lagrange dynamics (in blue) for mobile element 1 (robot forearm)

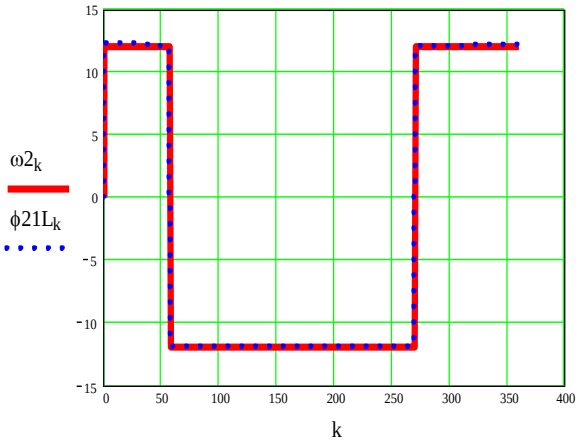

Fig. 7: The angular velocity (in red) compared to that of Lagrange dynamics (in blue) for mobile element 2 (arm)

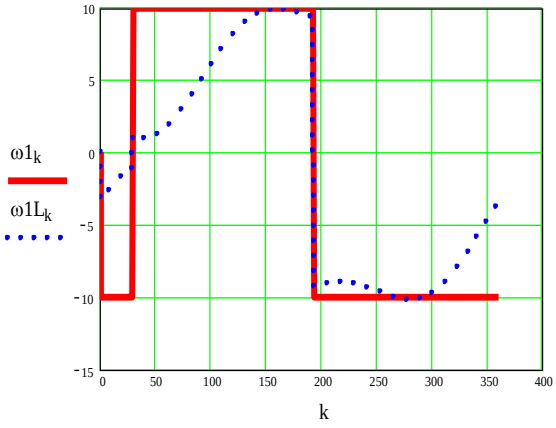

Fig. 8: The angular velocity (in red) versus that of the Lagrange dynamics plus the dynamics imposed by the internal couple B (in blue) for mobile element 1 (robot forearm)

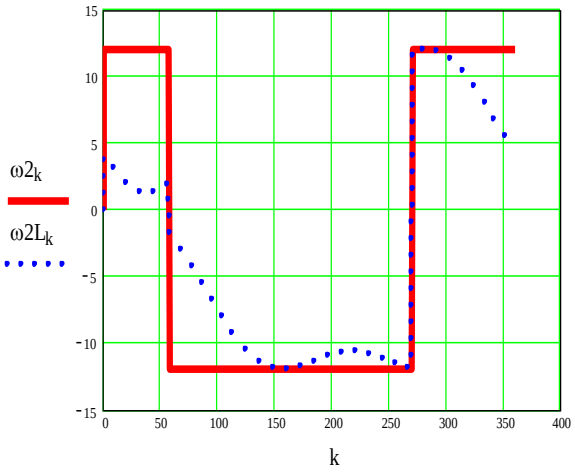

Fig. 9: The angular velocity (in red) versus that of the Lagrange dynamics plus the dynamics imposed by the internal couple B (in blue) for mobile element 2 (arm)

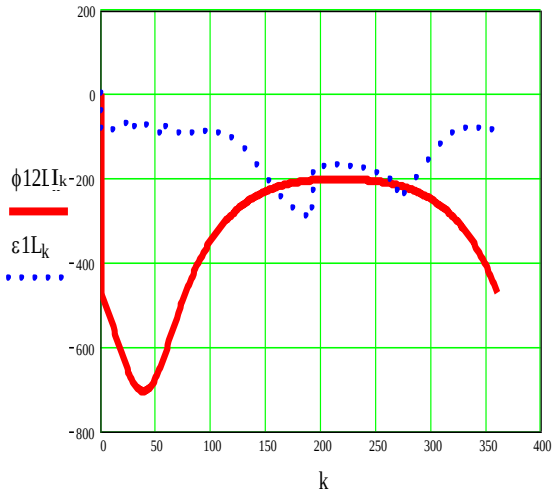

Fig. 10: The Lagrange II angular acceleration (in red) versus that of the Lagrange dynamics plus the dynamics imposed by the internal couple B (in blue) for mobile element 1 (robot forearm)

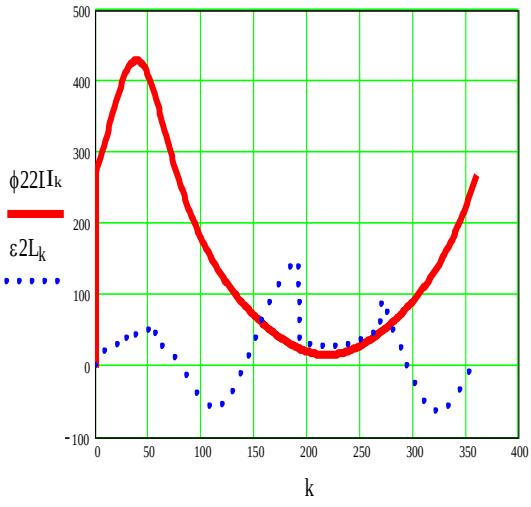

Fig. 11: The Lagrange II angular acceleration (in red) versus that of the Lagrange dynamics plus the dynamics imposed by the internal couple B (in blue) for mobile element 2 (arm)

Now, the Lagrange angular acceleration (ϕ_{12L} , or ϕ_{22L} in red) versus that of the Lagrange dynamics plus the dynamics imposed by the internal couple B (ε_{if} , or ω_{2L} in blue) will be shown for both, mobile element 1 (the robot's forearm; Fig. 10) and mobile element 2 (the arm; Fig. 11).

Next, the final (dynamic) angular accelerations (ω_{1L} , or ω_{2L}), obtained with Lagrange II plus the influence of the internal coupling B, will be presented in detail, both, for mobile element 1 (Fig. 12) and for mobile element 2 (Fig. 13).

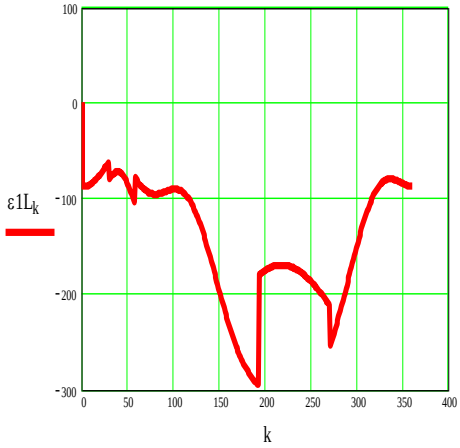

Fig. 12: The dynamic angular acceleration given by Lagrange II plus the dynamics imposed by the internal couple B for mobile element 1 (robot forearm)

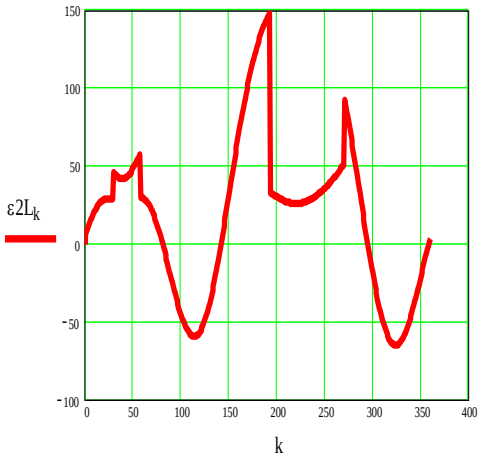

Fig. 13: The dynamic angular acceleration given by Lagrange II plus the dynamics imposed by the internal couple B for mobile element 2 (arm)

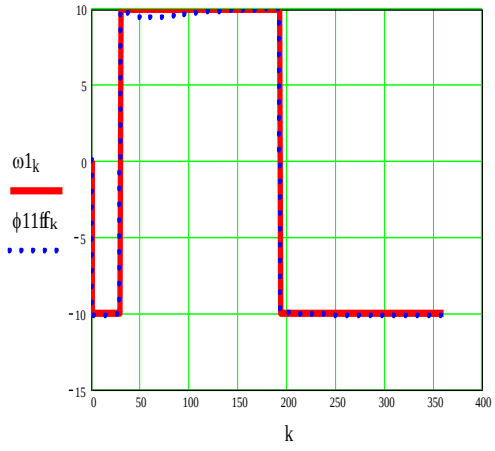

Fig. 14: The angular velocity (in red) compared to that of forces dynamics (in blue) for mobile element 1 (robot forearm)

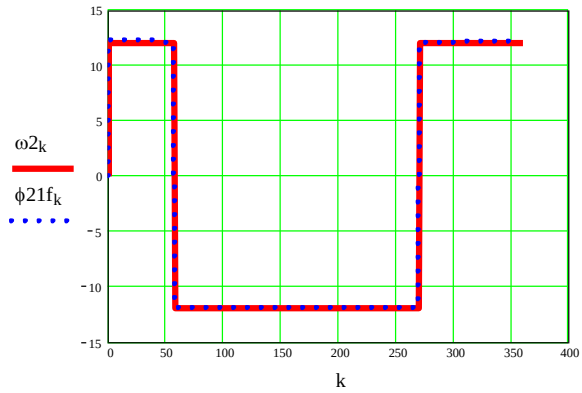

Fig. 15: The angular velocity (in red) compared to that of forces dynamics (in blue) for mobile element 2 (arm)

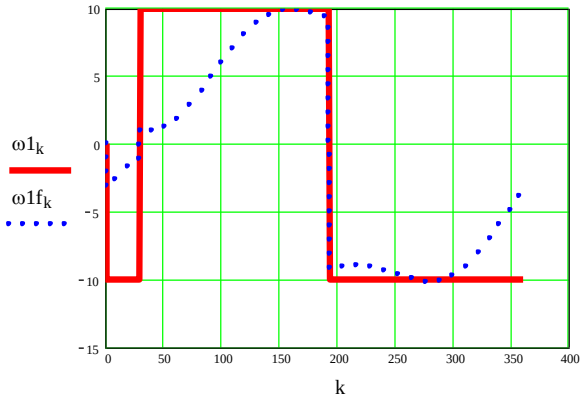

Fig. 16: The angular velocity (in red) versus that of the forces dynamics plus the dynamics imposed by the internal couple B (in blue) for mobile element 1 (robot forearm)

Forces Dynamics for A 3r Robot

The forces dynamics algorithm can be found in the appendix. Next, the results obtained with his help will be presented. The angular velocity (ω_1 or ω_2 in red) compared to that of forces dynamics (ϕ_{11f} , or ϕ_{21f} in blue) will be presented both for mobile element 1 (robot forearm; Fig. 14) and for mobile element 2 (arm; Fig. 15). The angular velocity (ω_1 or ω_2 in red) versus that of the forces dynamics plus the dynamics imposed by the internal couple B (ω_{1f} or ω_{2f} in blue) will be shown for both mobile element 1 (the robot's forearm; Fig. 16) and mobile element 2 (the arm; Fig. 17).

It can be seen (Figs 16-17) that the influence of the inner couple B is much greater than that of the external forces (obtained here with the help of Lagrange equations of the second order). In other words, the general dynamics is majorly influenced by the couple that connects the two elements in motion, and only in second place is the influence of the external forces that act on the robot (inertia forces, weights, technological resistances).

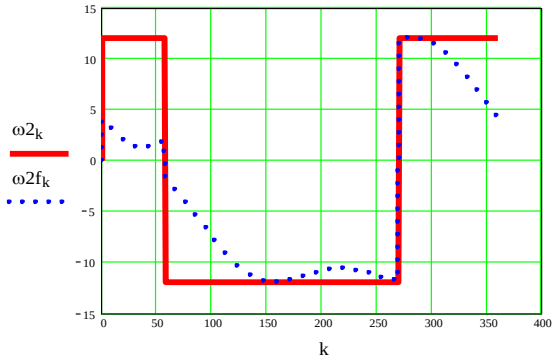

Fig. 17: The angular velocity (in red) versus that of the forces dynamics plus the dynamics imposed by the internal couple B (in blue) for mobile element 2 (arm)

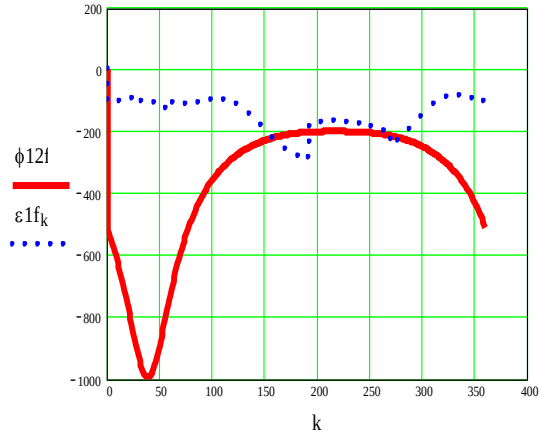

Fig. 18: The forces angular acceleration (in red) versus that of the forces dynamics plus the dynamics imposed by the internal couple B (in blue) for mobile element 1 (robot forearm)

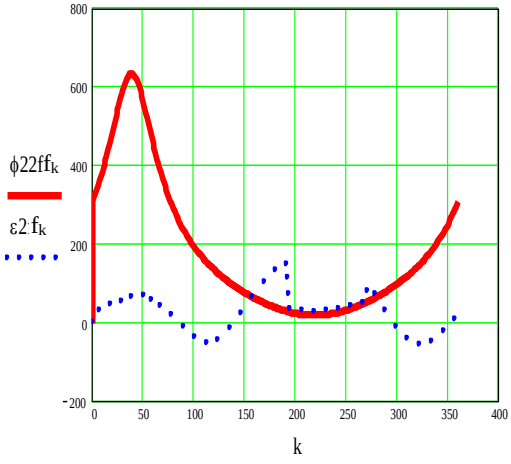

Fig. 19: The forces angular acceleration (in red) versus that of the forces dynamics plus the dynamics imposed by the internal couple B (in blue) for mobile element 2 (arm)

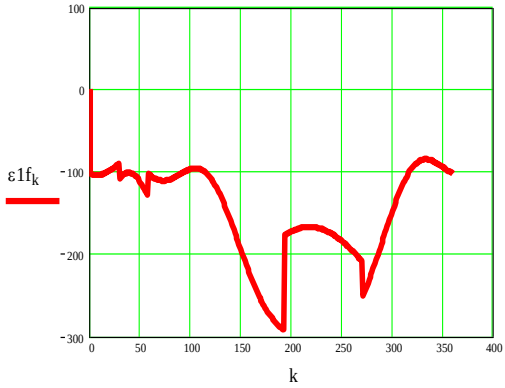

Fig. 20: The dynamic angular acceleration given by forces plus the dynamics imposed by the internal couple B for mobile element 1 (robot forearm)

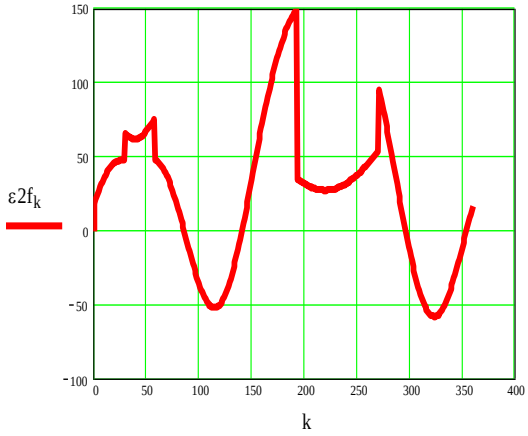

Fig. 21: The dynamic angular acceleration given by forces plus the dynamics imposed by the internal couple B for mobile element 2 (arm)

Now, the forces angular acceleration (ϕ_{12f} , or ϕ_{22f} in red) versus that of the forces dynamics plus the dynamics imposed by the internal couple B (ε_{1f} , or ω_1 in blue) will be shown for both, mobile element 1 (the robot's forearm; Fig. 18) and mobile element 2 (the arm; Fig. 19).

Next, the final (dynamic) angular accelerations (ε_{1f} , or ε_{2f}), obtained with forces plus the influence of the internal coupling B, will be presented in detail, both, for mobile element 1 (Fig. 20) and for mobile element 2 (Fig. 21).

Discussion

First of all, one will discuss the angular speed proposed at the first mobile element (motor) 1 (ω_1), compared to the dynamic Lagrange II speed (ϕ_{11L}) and with that obtained by superimposing the Lagrange II effects and the constrictions imposed by the internal coupling B ((ϕ_{11L}) Fig. 22).

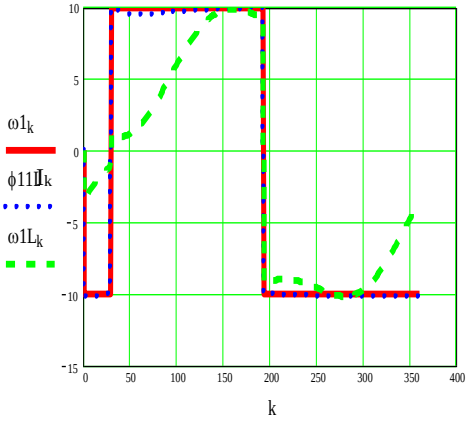

Fig. 22: The angular speed proposed at the first mobile element (motor) 1 (red), compared to the dynamic Lagrange II speed (blue), and with that obtained by superimposing the Lagrange II effects and the constrictions imposed by the internal coupling B (green)

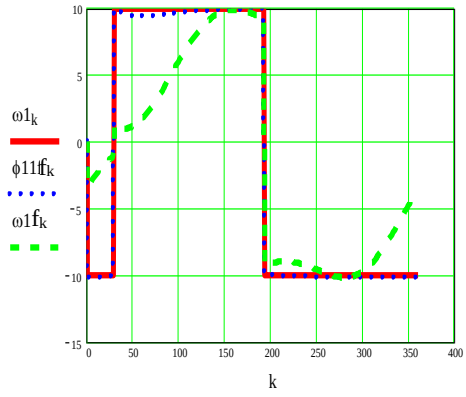

Fig. 23: The angular speed proposed at the first mobile element (motor) 1 (red), compared to the dynamic forces speed (blue), and with that obtained by superimposing the forces effects and the constrictions imposed by the internal coupling B (green)

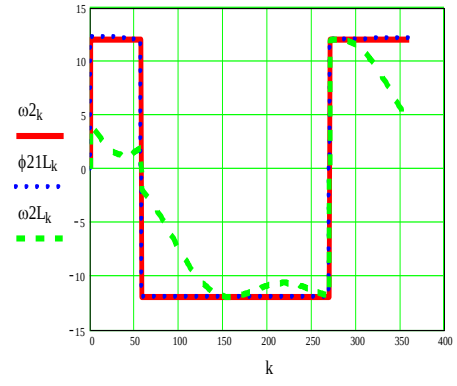

Fig. 24: The angular speed proposed at the second mobile element 2 (motors 1 + 2) (red), compared to the dynamic Lagrange II speed (blue), and with that obtained by superimposing the Lagrange II effects and the constrictions imposed by the internal coupling B (green)

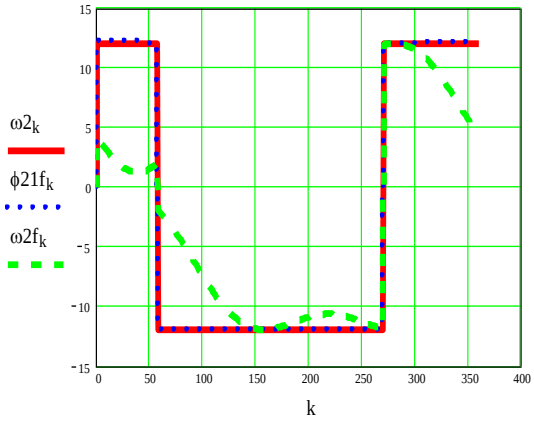

Fig. 25: The angular speed proposed at the second mobile element 2 (motors 1 + 2) (red), compared to the dynamic forces speed (blue), and with that obtained by superimposing the forces effects and the constrictions imposed by the internal coupling B (green)

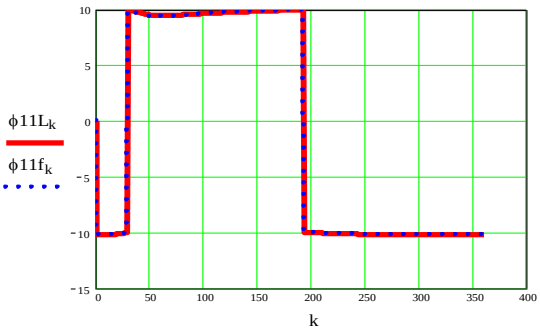

Fig. 26: The dynamic angular velocities obtained by the two different methods presented in the work, Lagrange type II (red) and forces (blue) for element 1, will be compared

Second, one will discuss the angular speed proposed at the first mobile element (motor) 1 (ω_1), compared to the dynamic forces speed (ϕ_{11f}) and with that obtained by superimposing the forces effects and the constrictions imposed by the internal coupling B ((ω_{1f}) Fig. 23).

One then repeats the procedure for mobile element 2 (engine 1 + engine 2), Figs. 24-25. Practically, the pivoting column that is missing from the presented scheme carries the entire robot, and element 1 also carries element 2, that is, motor 1 in coupling A actuates both element 1 and mobile element 2. Mobile element 2 rotates relative to mobile element 1 by motor 2 from coupling B, but the absolute rotation of mobile element 2 is due to the action of the two motors 1+2.

In the next step, the dynamic angular velocities are obtained by the two different methods presented in the work, Lagrange type II (ϕ_{11L}) and forces (ϕ_{11L}), for element 1 (Fig. 26) and for element 2 ($\phi_1 - \phi_2$) or (ϕ_{21f}) (Fig. 27) will be compared.

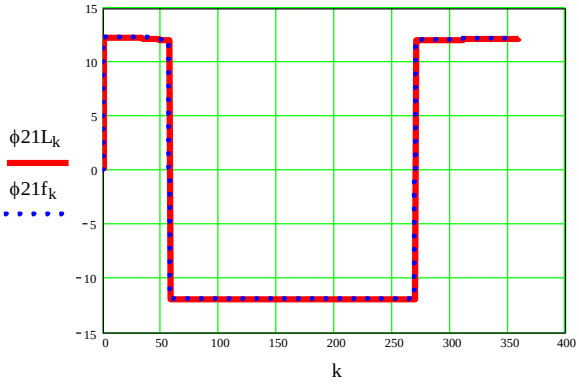

Fig. 27: The dynamic angular velocities obtained by the two different methods presented in the work, Lagrange type II (red) and forces (blue) for element 2, will be compared

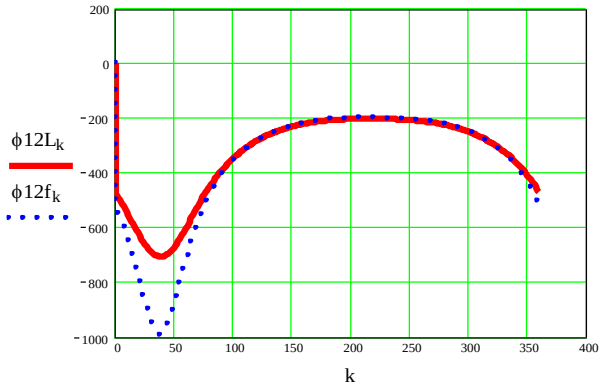

Fig. 28: The dynamic angular acceleration obtained by the two different methods presented in the work, Lagrange type II (red) and forces (blue) for element 1, will be compared

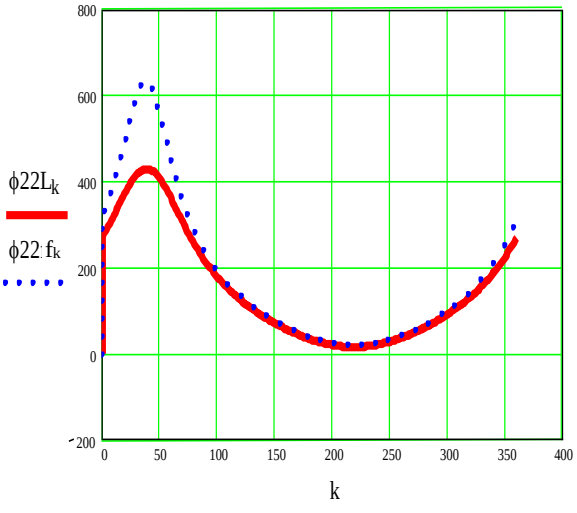

Fig. 29: The dynamic angular accelerations obtained by the two different methods presented in the work, Lagrange type II (red) and forces (blue) for element 2, will be compared

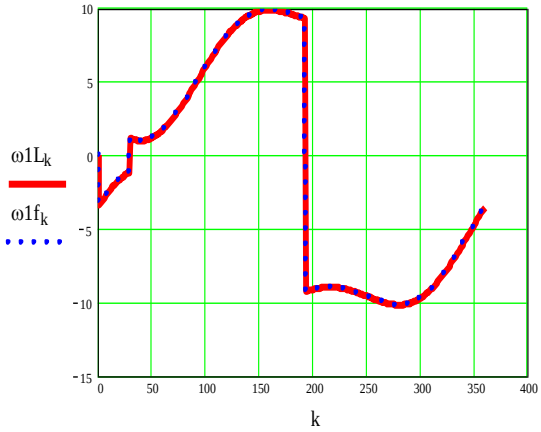

Fig. 30: The dynamic angular velocities obtained by the two different methods presented in the work, Lagrange type II (red) and forces (blue) effect which was superimposed with that of the constrictions imposed by the internal couple B for element 1, will

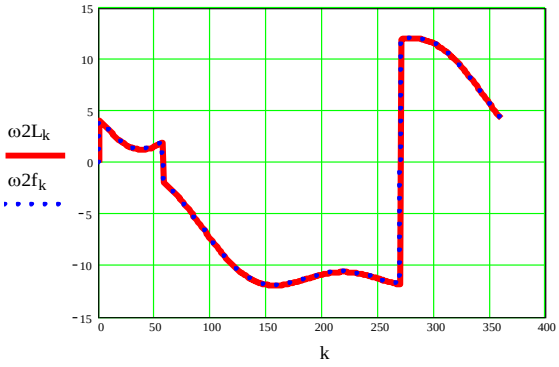

Fig. 31: The dynamic angular velocities obtained by the two different methods presented in the work, Lagrange type II (red) and forces (blue) effect which was superimposed with that of the constrictions imposed by the internal couple B for element 2, will be compared

Even if there are some differences, they are very small, thus showing the fact that both methods are valid.

One repeats the procedure for angular accelerations obtained with Lagrange II and those determined by the dynamic method of conservation of external forces acting on the 3 DoF robot (Figs. 28-29).

When one compares the angular accelerations obtained by the two totally different methods presented, it is obvious that the differences between the two methods are somewhat more visible, especially in the peak that appears on the first interval of the diagrams, having a sharper peak in the forces method.

Next, the comparative procedure between the two methods is repeated, but with the values considered final, at which the dynamic Lagrange II or force effect was superimposed with that of the constrictions imposed by the internal couple B (Figs. 30-33).

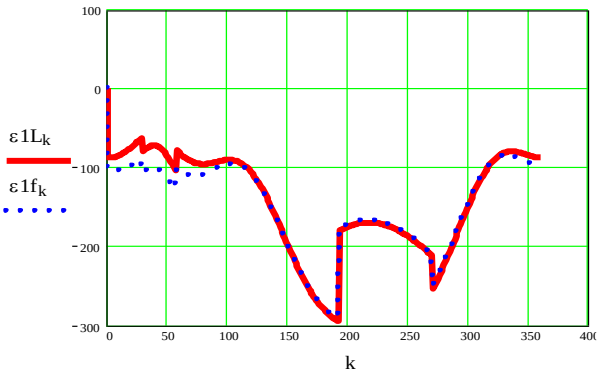

Fig. 32: The dynamic angular accelerations obtained by the two different methods presented in the work, Lagrange type II (red) and forces (blue) effect which was superimposed with that of the constrictions imposed by the internal couple B for element 1, will be compared

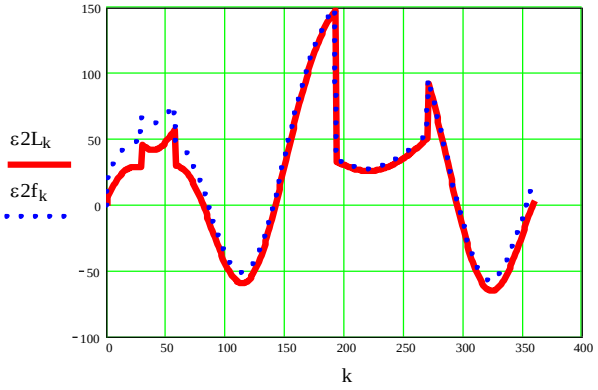

Fig. 33: The dynamic angular accelerations obtained by the two different methods presented in the work, Lagrange type II (red) and forces (blue) effect which was superimposed with that of the constrictions imposed by the internal couple B for element 2, will be compared

Even if there are some differences, they are very small, thus showing the fact that both methods are valid.

It is natural that for the accelerations (derived from the second order of the positions) small differences appear, but the two presented methods obviously remain valid. In general, both methods presented, in an original way, give conclusive results, close to each other, so that the simulations carried out in Mathcad constitute a first validation, precisely because of the similar results generated by two totally different methods (observe the totally different parameters of the two different systems of differential equations, Eqs. (7 and 12), respectively. To introduce the dynamic effects due to coupling B between the two mobile elements, it is necessary to correct (amplify) the angular velocity with a dynamic factor due to the coupling D_c. It differs depending on the type of coupling and for a fifth-class coupling (plane rotation) like the one used in 3 DoF robots, the value of the dynamic coefficient due to the C_5 coupling is $D_c = (\sin(\phi_1 - \phi_2))^2$ (Petrescu, 2012; 2014; 2022).

The advantages of both methods proposed in the paper compared to other known methods are their generality, the very high precision in the results obtained, the simplicity of the methods' application, and with Lagrange the advantage of a strong generalized character and the fact that the forces that must be taken into account no longer need to be precisely defined consideration, nor the accelerations of the centers of symmetry, for which only their scalar velocities are needed.

Conclusion

In the work, two completely different dynamic methods are presented, adapted by the author to an articulated robot based on 2 DoF. Both methodologies applied to the robot lead to credible and very close results (based on simulations carried out with the help of Mathcad Professional software), a fact that validates by itself both methods originally adapted and presented by the author.

The main advantage of the Lagrange method is the fact that the method uses the kinetic and potential energies of the concentrated masses present in the mechanism so that it is sufficient to express in each center of mass the coordinates of scalar positions with their derivatives of the 1st order (scalar velocities), unlike of the force method, which requires the expression of the scalar components of the inertial forces due to concentrated masses, forces that require scalar accelerations, i.e. the second-order derivatives of the respective centers' coordinates. Lagrange being the first scientist to introduce the dynamic effects of forces with the help of the study of total energies states that it is easier to determine the scalar coordinates of the centers of concentrated masses than to identify each external force separately.

Otherwise, today any specialist can write with great precision all the external forces that act on a machine so that the force method is no longer a dead end, it being easy enough and at hand. One thus has at our disposal two totally different methods that can be used comparatively.

To both methodologies proposed in the work, the dynamic effect produced by the internal link between the two mobile elements was added.

All simulations performed in Mathcad highlight similar results obtained by both proposed methods.

Acknowledgment

This text was acknowledged and appreciated by Dr. Veturia CHIROIU Honorific member of the Technical Sciences Academy of Romania (ASTR) Ph.D. supervisor in mechanical engineering.

Funding Information

Research contract: Contract number 36-5-4D/1986 from 24IV1985, beneficiary Romanian National Center for Science and Technology (RO CNST) improving dynamic mechanisms internal combustion engines.

Ethics

This article is original and contains unpublished material. The author declares that are no ethical issues and no conflict of interest that may arise after the publication of this manuscript.

References

Al Younes, Y., & Barczyk, M. (2021). Nonlinear model predictive horizon for optimal trajectory generation. *Robotics*, *10*(3), 90. https://doi.org/10.3390/robotics10030090

Alizade, R., Soltanov, S., & Hamidov, A. (2021). Structural synthesis of lower-class robot manipulators with general constraint one. *Robotics*, *10*(1), 14. https://doi.org/10.3390/robotics10010014

Arsenault, M., & Gosselin, C. M. (2006). Kinematic, static and dynamic analysis of a spatial three-degree-of-freedom tensegrity mechanism. https://doi.org/10.1115/1.2218881

Bandyopadhyay, S., & Ghosal, A. (2003, January). Analytical Determination of Principal Twists and Singular Directions in Robot Manipulators. In *International Design Engineering Technical Conferences and Computers and Information in Engineering Conference* (Vol. *37009*, pp. 1095-1106). https://doi.org/10.1115/DETC2003/DAC-48819

Besdo, D. (1973). Lagrange Equations of Second Kind. In: Examples to Extremum and Variational Principles in Mechanics. International Centre for Mechanical Sciences, vol *65*. Springer, Vienna. https://doi.org/10.1007/978-3-7091-2726-1_7

Caruso, M., Gallina, P., & Seriani, S. (2021). On the modelling of tethered mobile robots as redundant manipulators. *Robotics*, *10*(2), 81. https://doi.org/10.3390/robotics10020081

Chen, S., & Wen, J. T. (2021). Industrial robot trajectory tracking control using multi-layer neural networks trained by iterative learning control. *Robotics*, *10*(1), 50. https://doi.org/10.3390/robotics10010050

Colan, J., Nakanishi, J., Aoyama, T., & Hasegawa, Y. (2021). Optimization-based constrained trajectory generation for robot-assisted stitching in endonasal surgery. *Robotics*, *10*(1), 27. https://doi.org/10.3390/robotics10010027

Ebel, L. C., Maaß, J., Zuther, P., & Sheikhi, S. (2021). Trajectory Extrapolation for Manual Robot Remote Welding. *Robotics*, *10*(2), 77. https://doi.org/10.3390/robotics10020077

Engelbrecht, D., Steyn, N., & Djouani, K. (2021). Adaptive virtual impedance control of a mobile multi-robot system. *Robotics*, *10*(1), 19. https://doi.org/10.3390/robotics10010019

Essomba, T. (2021). Design of a five-degrees of freedom statically balanced mechanism with multi-directional functionality. *Robotics*, *10*(1), 11. https://doi.org/10.3390/robotics10010011

Fugal, J., Bae, J., & Poonawala, H. A. (2021). On the impact of gravity compensation on reinforcement learning in goal-reaching tasks for robotic manipulators. *Robotics*, *10*(1), 46. https://doi.org/10.3390/robotics10010046

Geng, J., Arakelian, V., Chablat, D., & Lemoine, P. (2021). Balancing of the Orthoglide taking into account its varying payload. *Robotics*, *10*(1), 30. https://doi.org/10.3390/robotics10010030

Giberti, H., Abbattista, T., Carnevale, M., Giagu, L., & Cristini, F. (2022). A methodology for flexible implementation of collaborative robots in smart manufacturing systems. *Robotics*, *11*(1), 9. https://doi.org/10.3390/robotics11010009

Gierlak, P. (2021). Adaptive position/force control of a robotic manipulator in contact with a flexible and uncertain environment. *Robotics*, *10*(1), 32. https://doi.org/10.3390/robotics10010032

Hao, L., Pagani, R., Beschi, M., & Legnani, G. (2021). Dynamic and friction parameters of an industrial robot: Identification, comparison and repetitiveness analysis. *Robotics*, *10*(1), 49. https://doi.org/10.3390/robotics10010049

Harrison, H. R. Nettleton, T. (1997). 2-Lagrange's Equations Advanced Engineering Dynam-ics, Butterworth-Heinemann, https://doi.org/10.1016/B978-034064571-0/50002-3

Liu, R., Nageotte, F., Zanne, P., de Mathelin, M., & Dresp-Langley, B. (2021). Deep reinforcement learning for the control of robotic manipulation: A focussed mini-review. *Robotics*, *10*(1), 22. https://doi.org/10.3390/robotics10010022

Maaroof, O. W., Dede, M. İ. C., & Aydin, L. (2021). A robot arm design optimization method by using a kinematic redundancy resolution technique. *Robotics*, *11*(1), 1. https://doi.org/10.3390/robotics11010001

Malik, A., Henderson, T., & Prazenica, R. (2021). Multi-objective swarm intelligence trajectory generation for a 7 degree of freedom robotic manipulator. *Robotics*, *10*(4), 127. https://doi.org/10.3390/robotics10040127

Medina, O., & Hacohen, S. (2021). Overcoming kinematic singularities for motion control in a caster wheeled omnidirectional robot. *Robotics*, *10*(4), 133. https://doi.org/10.3390/robotics10040133

Miguel-Tomé, S. (2021). The Heuristic of Directional Qualitative Semantic: A New Heuristic for Making Decisions about Spinning with Qualitative Reasoning. *Robotics*, *10*(1), 17. https://doi.org/10.3390/robotics10010017

Oliveira, A. R. (2013). Lagrange as a Historian of Mechanics. *Advances in Historical Studies*, *2*(03), 126-130. https://doi.org/10.4236/ahs.2013.23016

Pacheco-Gutierrez, S., Niu, H., Caliskanelli, I., & Skilton, R. (2021). A multiple level-of-detail 3rd data transmission approach for low-latency remote visualisation in teleoperation tasks. *Robotics*, *10*(3), 89. https://doi.org/10.3390/robotics10030089

Palomba, I., Gualtieri, L., Rojas, R., Rauch, E., Vidoni, R., & Ghedin, A. (2021). Mechatronic re-design of a manual assembly workstation into a collaborative one for wire harness assemblies. *Robotics*, *10*(1), 43. https://doi.org/10.3390/robotics10010043

Pennestri, E., Cavacece, M., & Vita, L. (2005, January). On the computation of degrees-of-freedom: a didactic perspective. In *International Design Engineering Technical Conferences and Computers and Information in Engineering Conference* (Vol. *47438*, pp. 1733-1741). https://doi.org/10.1115/DETC2005-84109

Petrescu, F. I. T. (2022). Advanced Dynamics Processes Applied to an Articulated Robot. *Processes*, *10*(4), 640. https://doi.org/10.3390/pr10040640

Petrescu, F. I. T. (2012b). Theory of Mechanisms: Course and Applications, CreateSpace Independent Publishing Platform (September 12, 2012), Romanian Paperback, pp: 286. ISBN-10: 1479302333. https://www.amazon.com/gp/product/1479302333

Petrescu, F. I. T., (2014a). Serial Mechatronic Systems, Parallel and Mixed, 12 February 2014, Create Space Publisher, Romanian, pp: 226. ISBN-10: 1495923819.

Petrescu, F. I. T., & Petrescu, R. V. V. (2021). Direct kinematics of a manipulator with three mobilities. *Independent Journal of Management & Production*, *12*(7), 1875-1900. https://doi.org/10.14807/ijmp.v12i7.1160

Petrescu, F. I., & Petrescu, R. V. (2016). Dynamic cinematic to a structure 2R. *GEINTEC Journal*, *6*(2). https://doi.org/10.7198/geintec.v6i2.371

Pozzi, M., Prattichizzo, D., & Malvezzi, M. (2021). Accessible educational resources for teaching and learning robotics. *Robotics*, *10*(1), 38. https://doi.org/10.3390/robotics10010038

Raviola, A., Guida, R., De Martin, A., Pastorelli, S., Mauro, S., & Sorli, M. (2021). Effects of temperature and mounting configuration on the dynamic parameters identification of industrial robots. *Robotics*, *10*(3), 83. https://doi.org/10.3390/robotics10030083

Scalera, L., Seriani, S., Gallina, P., Lentini, M., & Gasparetto, A. (2021). Human–robot interaction through eye tracking for artistic drawing. *Robotics*, *10*(2), 54. https://doi.org/10.3390/robotics10020054

Stodola, M., Rajchl, M., Brablc, M., Frolík, S., & Křivánek, V. (2021). Maxwell Points of Dynamical Control Systems Based on Vertical Rolling Disc-Numerical Solutions. *Robotics*, *10*(3), 88. https://doi.org/10.3390/robotics10030088

Stuhlenmiller, F., Weyand, S., Jungblut, J., Schebek, L., Clever, D., & Rinderknecht, S. (2021). Impact of cycle time and payload of an industrial robot on resource efficiency. *Robotics*, *10*(1), 33. https://doi.org/10.3390/robotics10010033

Sun, J., Han, X., Li, T., & Li, S. (2021). Dynamic Parameter Identification of a Pointing Mechanism Considering the Joint Clearance. *Robotics*, *10*(1), 36. https://doi.org/10.3390/robotics10010036

Thompson, L. A., Badache, M., Brusamolin, J. A. R., Savadkoohi, M., Guise, J., Paiva, G. V. D., ... & Shetty, D. (2021). Multidirectional overground robotic training leads to improvements in balance in older adults. *Robotics*, *10*(3), 101. https://doi.org/10.3390/robotics10030101

Vatsal, V., & Hoffman, G. (2021). The wearable robotic forearm: design and predictive control of a collaborative supernumerary robot. *Robotics*, *10*(3), 91. https://doi.org/10.3390/robotics10030091

Yamakawa, Y., Katsuki, Y., Watanabe, Y., & Ishikawa, M. (2021). Development of a high-speed, low-latency telemanipulated robot hand system. *Robotics*, *10*(1), 41. https://doi.org/10.3390/robotics10010041

Appendix

Dynamics based on forces and Lagrange II dynamics, for a 3R robot in inverse kinematics:

$$Is := 3 \qquad ID := 5$$
$$I1 := I\,S \qquad I2 := ID\,r := 1.5$$
$$XD := 5 \quad YD := \quad 4 \quad XA := 0$$
$$YA := 0 \qquad Is1 := \frac{I1}{3}$$
$$Is2\,\frac{I2}{3} \qquad k := 0..360$$
$$\alpha_k := 2 \cdot \qquad \pi \cdot \frac{k}{360}$$
$$ml := I1 \qquad m2 := 5 \cdot$$
$$I2\,RT := I2 \qquad RT := -2500$$
$$g := 9.81 \qquad mC := \frac{|RT|}{g}$$
$$XC_k := XD + r \cdot \cos(\alpha_k)$$
$$YC_k := YD + r \cdot \sin(\alpha_k)$$

$$I_k := \sqrt{(XC_k - XA)^2 + (YC - YA)^2}$$
$$YB := YA + \frac{YC_k \cdot \left[(I_k)^2 + IS^2 - ID^2\right] + XC_k \cdot \sqrt{4.(I_k)^2 \cdot IS^2 - \left[(I_k)^2 . IS^2 - ID^2\right]^2}}{2.(I_k)^2}$$
$$XB_k := XA + if\left[XC_k = 0, \sqrt{IS^2} - (YB_k - YA)^2\right], \frac{(I_k)^2 + IS^2 - ID^2 - 2 \cdot YC_k \cdot YB_k}{2.XC_k}$$
$$cI_k := \frac{(XB_k - XA)}{I1}$$
$$s1_k := \frac{(YB_k - YA)}{I1}$$
$$\phi 1_k := sign(s1_k) \cdot a\cos(c1_k)$$
$$c2_k := \frac{(XC_k - XB_k)}{I2}$$
$$s2_k := \frac{YX_k - YB_k}{I2}$$
$$\phi 2_k := sign(s2_k) \cdot a\cos(c2_k)$$

Selection and automation of motor speeds, when we want constant speeds for the two elements 1 and 2 Note motor 1 rotates at the angle FI1 with the speed $\omega 1$ motor 2 rotates with FI2-FI1, with speed $\omega 2 - \omega 1$.

$$w1 := 10$$
$$\omega 1_k := if\left(k < 1,0, w1 \cdot sign\left(\phi 1_k - \phi 1_{k-1}\right)\right)$$
$$\varepsilon 1_k := if\left(k < 1,0, \omega 1_k \cdot \frac{\omega 1_k - \omega 1_{k-1}}{\phi 1_k}\right)$$
$$w2 := 12$$
$$\omega 2_k := if\left(k < 1,0, w2 \cdot sign\left(\phi 2_k - \phi 2_{k-1}\right)\right)$$
$$\varepsilon 2_k := if\left(k < 1,0, \omega 2_k \cdot \frac{\omega 2_k - \omega 2_{k-1}}{\phi 2_k}\right)$$

Dynamics Due to Forces

$$f11_k := (m1 \cdot Is1 + m2 \cdot I1 + mC \cdot I1) \cdot \sin(\phi 1_k)$$
$$f12_k := (m2 \cdot Is2 + mC \cdot I2) \cdot \sin(\phi 2_k)$$
$$f21_k := (m1 \cdot Is1 + m2 \cdot I1 + mC \cdot I1) \cdot \cos(\phi 1_k)$$
$$f22_k := (m2 \cdot Is2 + mC \cdot I2) \cdot \cos(\phi 2_k)$$
$$f1_k := f21_k \cdot (\omega 1_k)^2 - f22_k \cdot (\omega 2_k)^2$$
$$f2_k := f11_k \cdot (\omega 1_k)^2 - f12_k \cdot (\omega 2_k)^2 - g \cdot (m1 + m2 + mC)$$

$$Dc_k := \left(\sin(\phi 2_k)\right)^2$$
$$\Delta f_k := f11_k - f12_k \cdot f21_k$$
$$\Delta f1_k := f22_k - f12_k \cdot f2_k$$
$$\Delta f2_k := f11_k \cdot f2_k - f1_k \cdot f21_k$$
$$\phi 12\,f_k := \frac{\Delta f1_k}{\Delta f_k}$$
$$\phi 22\,f_k := \frac{\Delta f2_k}{\Delta f_k}$$
$$\Delta \phi 11\,f_k := \quad if\left[k < 1,0, \phi 12\,f_k \cdot \frac{\phi 1_k - \phi 1_{k-1}}{\omega 1_k}\right]$$
$$\phi 11\,f_k := \omega 1_k + \Delta \phi 11\,f_k$$
$$\omega 1\,f_k := \phi 11\,f_k \cdot Dc_k$$
$$\Delta \phi 21\,f_k ;= if\left[k < 1,0, \phi 22\,f_k \cdot \frac{\left(\phi 2_k - \phi 2_{k-1}\right)}{\omega 2_k}\right]$$
$$\phi 21\,f_k := \omega 2_k + \Delta 21\,f_k$$
$$\omega 2\,f_k := \phi 21\,f_k \cdot Dc_k$$
$$Dc1\,f_k ;= \sin\left[2 \cdot \left(\phi 1_k - \phi 2_k\right)\right] \cdot \left(\omega 1\,f_k - \omega 2\,f_k\right)$$
$$\varepsilon 1\,f_k := \phi 12\,f_k \cdot Dc_k + \phi 11\,f_k \cdot Dc1\,f_k$$
$$\varepsilon 2\,f_k = \phi 22\,f_k \cdot Dc_k + \phi 21\,f_k \cdot Dc1\,f_k$$

Lagrange Dynamics II

$$Ig11_k := m1 \cdot Is1^2 + m2 \cdot I1^2 + mC \cdot I1^2$$

$$Ig12_k := \left(m2 \cdot Is2 + mC \cdot I2\right) + I1 \cdot \cos\left(\phi 1_k - \phi 2_k\right)$$

$$Ig21_k := Ig12_k :=$$

$$Ig22_k := m2 \cdot Is2^2 + mC \cdot I2^2$$

$$Ig1_k := -\left(m2 \cdot Is2 + mC \cdot I2\right) +$$

$$I1 \cdot \sin\left(\phi 1_k - \phi 2_k\right) \cdot \left(\omega 2_k\right)^2 -$$

$$\left(m1 \cdot Is1 + \cdot I1 + mC \cdot I1\right) \cdot g \cdot \cos\left(\phi 1_k\right)$$

$$Ig2_k := -\left(m2 \cdot Is2 + mC \cdot I2\right) +$$

$$I1 \cdot \sin\left(\phi 1_k - \phi 2_k\right) \cdot \left(\omega 2_k\right)^2 -$$

$$\left(m2 \cdot Is2 + mC \cdot I2\right) \cdot g \cdot \cos\left(\phi 2_k\right)$$

$$\Delta L_k := Ig22_k - Ig12_k \cdot Ig21_k$$

$$\Delta L1_k := Ig1_k \cdot Ig22_k - Ig12_k \cdot Ig2_k$$

$$\Delta L2_k := Ig11_k \cdot Ig2_k - Ig1_k \cdot Ig21_k$$

$$\phi 12L_k := \frac{\Delta L1_k}{\Delta L_k} \phi 22L_k; = \frac{\Delta L2_k}{\Delta L_k}$$

$$\Delta \omega 1L_k := if\left[\omega 1_k = 0, 0, \frac{\phi 12L_k}{\omega 1_k} \cdot \left(\phi 1_k - \phi 1_{k-1}\right)\right]$$

$$\phi 11L_k := \omega 1_k + \Delta \omega 1L_k \quad \omega 1L_k := \phi 11L_k \cdot Dc_k$$

$$\Delta \omega 2L_k := if\left[\omega 2_k = 0, 0, \frac{\phi 22L_k}{\omega 2_k} \cdot \left(\phi 2_k - \phi 2_{k-1}\right)\right]$$

$$\phi 21L_k := \omega 2_k + \Delta \omega 2L_k \quad \omega 2L_k := \phi 21L_k \cdot Dc_k$$

$$Dc1L_k := \sin\left[2 \cdot \left(\phi 1_k - \phi 2_k\right)\right] \cdot \left(\omega 1L_k - \omega 2L_k\right)$$

$$\varepsilon 1L_k := \phi 12L_k \cdot Dc_k + \phi 11L_k \cdot Dc1L_k$$

$$\varepsilon 2L_k := \phi 22L_k \cdot Dc_k + \phi 21L_k \cdot Dc1L_k$$